Response of light drip line nuclei to spin dependent operators

I. Hamamoto[1] and H. Sagawa[1,2]
[1]*Department of Mathematical Physics, Lund Institute of Technology at University of Lund, Lund, Sweden*
[2]*Center for Mathematical Sciences, University of Aizu, Ikki-machi, Aizu-Wakamatsu, Fukushima 965, Japan*
(Received 28 July 1999; published 15 November 1999)

The response of light drip line nuclei to spin-isospin dependent fields is investigated, using the self-consistent Hartree-Fock plus the random-phase approximation with Skyrme interactions. Including simultaneously both the isoscalar and isovector spin correlation, the random-phase-approximation response function is estimated in the coordinate space so as to take properly into account the continuum effect. The spin-orbit splitting, which plays an essential role in the spin-dependent response functions, is examined as a function of the mass number when we approach the drip line nuclei. It is found that the calculated $M1$ peaks in ${}^{8}_{6}C_{2}$ and ${}^{8}_{2}He_{6}$ are much lower in energy than those expected from our knowledge of the β-stable nucleus ${}^{12}_{6}C_{6}$. [S0556-2813(99)02212-8]

PACS number(s): 21.60.Jz, 23.20.Js, 27.20.+n, 27.30.+t

I. INTRODUCTION

In connection with the recent development of facilities of radioactive nuclear ion beams all over the world, dynamics of nuclei far from β stability lines has become a very popular research field. The presence of nucleons, which have separation energies drastically smaller than those in traditional β-stable nuclei, together with the exotic ratio of Z/N for a given mass number, which produces a large difference between the Fermi level of neutrons and that of protons, leads to very interesting and unexpected phenomena. Performing the Hartree-Fock (HF) calculation with Skyrme interactions and then using the random-phase approximation (RPA), we have studied the response functions of drip line nuclei to spin independent fields [1]; see also Refs. [2] and [3].

The dynamical response of drip line nuclei to spin dependent fields is expected to show also the interesting exotic structure, exhibiting the low-lying threshold strength unique in those nuclei. Taking into account both the isoscalar (IS) and isovector (IV) spin correlation in the self-consistent RPA with Skyrme interactions, which is solved in the coordinate space with the Green's function method, we study the response functions of light drip line nuclei to spin dependent fields and the magnetic dipole ($M1$) field.

The structure of the nuclear response to spin dependent dipole fields depends sensitively on the spin-orbit potential. Moreover, it is an interesting question to study how the spin-orbit energy splitting changes as a function of the mass number when we approach the drip line nuclei. The spin-orbit potential of the simple form [4]

$$V_{ls}(r)=V_{ls}\,r_0^2\,(\vec{l}\cdot\vec{s})\,\frac{1}{r}\,\frac{\partial}{\partial r}f(r) \tag{1}$$

is often used, where V_{ls} is a constant and r_0 is the radius parameter with the nuclear radius $R=r_0A^{1/3}$, while $f(r)$ expresses a radial function of either the density or the central real potential. Then, the spin-orbit energy splitting of the largest l orbitals in the occupied outermost major shell is approximately proportional to $A^{-1/3}$. This is because the l value is proportional to $A^{1/3}$, while the expectation value of $R(\partial/\partial r)f(r)$ is fairly independent of the particular orbit for nucleons bound by about 10 MeV [4]. On the other hand, the observed spin-orbit energy splitting of the largest l orbitals is known to be almost A independent going from ^{16}O to ^{208}Pb. Thus the mass-number dependence of the spin-orbit energy splitting is not yet well understood from a theoretical point of view. Furthermore, it is an open question how the spin-orbit splitting changes in very light nuclei.

The spin-orbit splitting for low l orbitals is expected to decrease appreciably as the binding energies of the orbitals approach zero. First, we take the potential without a diffused surface. In Ref. [5] it is shown that for a square-well potential [that is, taking $f(r)$ to be a step function at the nuclear surface] the expectation value

$$\langle nl|R\,\frac{\partial}{\partial r}f(r)|nl\rangle \tag{2}$$

for $l=0$ goes to zero in the limit that the binding energy of the (nl) particle approaches zero. On the other hand, in the same limit the value for $l=1$ becomes about a half of that for the particles with the binding energy of 10 MeV, while there is no such drastic effect for $l>2$. The decrease of the probability of one-particle wave functions with low l values around the nuclear surface makes the expectation value (2) smaller and thus the spin-orbit splitting smaller. Second, it is found that for neutrons with energies $\epsilon\gtrsim -1$ MeV in HF calculations the one-particle levels with lower angular momenta are appreciably pushed down relative to those with higher angular momenta [6]. This is because the wave functions of the orbitals with lower angular momenta can easily extend to the outside the nuclear surface and, consequently, the kinetic energies of the orbitals decrease. The presence of a diffused surface in the nuclear potential further helps the extension of those wave functions and thereby the lowering of those energy eigenvalues. At the same time, the extended wave functions can make use of the tail of the attractive potential. See also Ref. [7]. When a pair of spin-orbit partner levels approach being unbound, the higher-lying level with $j=l-\frac{1}{2}$ is pushed down more strongly than the lower-lying one with $j=l+\frac{1}{2}$. Thus the presence of a diffused surface in

the nuclear potential contributes further to decrease the spin-orbit splitting for low l orbitals as the binding energies approach zero.

The argument described above can be applicable also to one-particle resonant levels with small widths, since inside nuclei the behavior of wave functions of those resonant states is similar to that of one-particle bound states with small binding energies.

From the previous study of the response functions to spin-independent fields it is known that particles with smaller orbital angular momenta l in drip line nuclei are particularly efficient in producing an appreciable amount of low-lying threshold strength. Since $s_{1/2}$ orbitals have no spin-orbit partners, in the present work we concentrate mainly on the study of spin excitations of $l=1$ particles in light drip line nuclei. In Sec. II the model and the necessary formulas are described. In Sec. III the HF one-particle level scheme, in particular, the spin-orbit energy splitting of C isotopes from ${}^{8}_{6}\mathrm{C}_2$ to ${}^{22}_{6}\mathrm{C}_{16}$ is examined. In Sec. IV the magnetic dipole excitations of the $A=8$ mirror nuclei, the neutron drip line nucleus ${}^{8}_{6}\mathrm{C}_2$, and the proton drip line nucleus ${}^{8}_{2}\mathrm{He}_6$ are studied and compared. In Sec. V the spin-isospin and magnetic dipole excitations in the neutron drip line nucleus ${}^{22}_{6}\mathrm{C}_{16}$ are investigated. In Sec. VI the discussion and conclusion are given.

II. MODEL AND FORMULATION

As a microscopic model, we perform the self-consistent HF+RPA calculations with Skyrme interactions [8]. The RPA equations are solved in the coordinate space with the Green's function method in order to take into account properly the coupling to the continuum [9,10]. Both the IS and IV spin correlations are taken into account simultaneously, which is particularly important to study the response in nuclei near drip lines.

The RPA Green's function G^{RPA} is expressed as a Lippmann-Schwinger type equation

$$G^{\mathrm{RPA}}=G^{(0)}+G^{(0)}v_{ph}G^{\mathrm{RPA}}=(1-G^{(0)}v_{ph})^{-1}G^{(0)}, \quad (3)$$

where v_{ph} is the residual particle-hole (p-h) interaction. The unperturbed Green's function $G^{(0)}$ is defined in a closed form:

$$G^{(0)}(\vec{r},\vec{r}\,':\omega)=\sum_h \varphi_h^*(\vec{r})\langle\vec{r}|\frac{1}{H_0-\epsilon_h-\omega-i\eta} + \frac{1}{H_0-\epsilon_h+\omega-i\eta}|\vec{r}\,'\rangle\varphi_h(\vec{r}\,') \quad (4)$$

with the HF Hamiltonian H_0. The inverse operator expression in Eq. (4) is nothing but one-body Green's function and can be expressed by a product of two solutions (regular and irregular solutions) of the operator equation in the denominator [9,10]. The p-h interaction v_{ph} is derived from the Hamiltonian density $\langle H\rangle$ of Skyrme interaction by so-called Landau procedure,

$$\begin{aligned} v_{ph}(\vec{r},\vec{r}\,')&=\sum_{s=0}^{1}\sum_{t=0}^{1}\frac{1+\vec{\sigma}\cdot\vec{\sigma}\,'+(-1)^s(1-\vec{\sigma}\cdot\vec{\sigma}\,')}{2} \times\frac{1+\vec{\tau}\cdot\vec{\tau}\,'+(-1)^t(1-\vec{\tau}\cdot\vec{\tau}\,')}{2}\frac{\delta^2\langle H\rangle}{\delta\rho_{\tau\sigma}\delta\rho_{\tau'\sigma'}} \\ &=\{a+b(\vec{\nabla}_p^2+\vec{\nabla}_h^2+\vec{\nabla}_p^2+\vec{\nabla}_h^2) \\ &\quad +b(\vec{\nabla}_p-\vec{\nabla}_h)\cdot(\vec{\nabla}_p-\vec{\nabla}_h) \\ &\quad +c(\vec{\nabla}_p+\vec{\nabla}_h)\cdot(\vec{\nabla}_p+\vec{\nabla}_h)\}\delta(\vec{r}-\vec{r}\,'), \end{aligned} \quad (5)$$

where the coefficients a, b, and c are functions of Skyrme parameters:

$$\begin{aligned} a&=\frac{3}{4}t_0+\frac{1}{16}(\alpha+2)(\alpha+1)t_3\rho^\alpha \\ &\quad -\frac{1}{48}t_3(1+2x_3)\alpha(\alpha-1)\frac{(\rho_n-\rho_p)^2}{\rho^2}\rho^\alpha \\ &\quad -\left[\frac{1}{4}t_0(1+2x_0)+\frac{1}{24}t_3(1+2x_3)\rho^\alpha\right]\vec{\tau}\cdot\vec{\tau}\,' \\ &\quad -\left[\frac{1}{4}t_0(1-2x_0)+\frac{1}{24}t_3(1-2x_3)\rho^\alpha\right]\vec{\sigma}\cdot\vec{\sigma}\,' \\ &\quad -\left[\frac{1}{4}t_0+\frac{1}{24}t_3\rho^\alpha\right]\vec{\sigma}\cdot\vec{\sigma}\,'\vec{\tau}\cdot\vec{\tau}\,', \end{aligned} \quad (6)$$

$$\begin{aligned} b&=-\frac{1}{32}\{3t_1+t_2(5+4x_2) \\ &\quad +[t_2(1+2x_2)-t_1(1+2x_1)]\vec{\tau}\cdot\vec{\tau}\,' \\ &\quad +[t_2(1+2x_2)-t_1(1-2x_1)]\vec{\sigma}\cdot\vec{\sigma}\,' \\ &\quad +(t_2-t_1)\vec{\sigma}\cdot\vec{\sigma}\,'\vec{\tau}\cdot\vec{\tau}\,'\}, \end{aligned} \quad (7)$$

$$\begin{aligned} c&=\frac{1}{32}\{3t_1-t_2(15+12x_2) \\ &\quad -[t_1(1+2x_1)+3t_2(1+2x_2)]\vec{\tau}\cdot\vec{\tau}\,' \\ &\quad -[t_1(1-2x_1)+3t_2(1+2x_2)]\vec{\sigma}\cdot\vec{\sigma}\,' \\ &\quad -(t_1+3t_2)\vec{\sigma}\cdot\vec{\sigma}\,'\vec{\tau}\cdot\vec{\tau}\,'\}. \end{aligned} \quad (8)$$

The spin-dependent p-h interactions depend on the operators $\vec{\sigma},\vec{\sigma}(\vec{\nabla}_p^2+\vec{\nabla}_h^2)$ and $\vec{\sigma}\cdot(\vec{\nabla}_p\pm\vec{\nabla}_h)$. For the numerical representation of the Green's function $G^{(0)}(\vec{r},\vec{r}\,':\omega)$, we will propagate these spin-dependent operators as well as the gradient operator $(\vec{\nabla}_p-\vec{\nabla}_h)$, which is needed for calculating the magnetic orbital strength. In the present calculation the neutron and proton degree of freedom are explicitly introduced in the RPA Green's function (3) including the IS and IV spin-dependent interactions simultaneously. Then, the matrix dimension of the $G^{(0)}(\vec{r},\vec{r}\,':\omega)$ will be doubled for each

propagated operator in the coordinate space. The explicit account of the proton and neutron degree of freedom should be taken in the Green's function with the IS and IV correlations in order to study the coupling and/or decoupling of the IS and IV mode of spin excitations. In this paper we study the response to the magnetic dipole operator as well as to the spin and spin-isospin operators. The magnetic dipole operator is defined as

$$O(M1)=\sum_i \sqrt{\frac{3}{4\pi}}[g_s(i)\vec{s}_i+g_l(i)\vec{l}_i], \tag{9}$$

where the spin and orbital g factors are given by

$$g_s(g_l)=\begin{cases}5.58 & (1) \quad \text{for protons}\\ -3.82 & (0) \quad \text{for neutrons}\end{cases} \tag{10}$$

in units of $\mu=e\hbar/2m_pc$. The spin and spin-isospin operators are defined as

$$O(\text{spin})=\sum_i \vec{\sigma}_i, \tag{11}$$

$$O(\text{spin-isospin})=\sum_i \vec{\sigma}_i\tau_{zi}. \tag{12}$$

The transition strength $S(\omega)$ for the states above the threshold can be obtained from the imaginary part of G^{RPA} as

$$S(\omega)\equiv \sum_n |\langle n|O(\vec{\sigma},\vec{l})|0\rangle|^2\delta(E-E_n)$$

$$=\frac{1}{\pi}\text{Im}\{\text{Tr}[O(\vec{\sigma},\vec{l})G^{RPA}(\vec{\sigma},\vec{l};\vec{\sigma}',\vec{l}';\omega)O(\vec{\sigma}',\vec{l}')]\}, \tag{13}$$

while the strength below the threshold is calculated from the residue of the pole in the real part of the response function. The transition operators (9), (11), and (12) can be expressed by a linear combination of spin operators $\sigma_0,\sigma_{\pm1}$ and the gradient operator $\nabla_{\pm1}$ in the helicity representation taking the intrinsic z axis as the quantization axis [11,8]. Then, for example, the transition strength $S(\omega)$ for the $M1$ operator is evaluated by the sum of responses of the RPA Green's function to the operators σ_0, σ_1, and ∇_1 . The responses to the σ_{-1} and ∇_{-1} operators can be obtained from those of σ_1 and ∇_1, respectively, due to the symmetry of the Green's function. The Galilean noninvariant term $(\vec{\nabla}_p+\vec{\nabla}_h)\cdot(\vec{\nabla}_p+\vec{\nabla}_h)$ in the interaction v_{ph} is discarded in the following calculations to decrease the number of perturbations for the RPA Green's functions. It is known that these Galilean noninvariant terms have a minor contribution to the p-h matrix elements and are often dropped out of the RPA response [8]. In the plane wave approximation which is assumed for the calculations of the Landau-Migdal parameters, these terms disappear due to a cancellation between p and h channels [12].

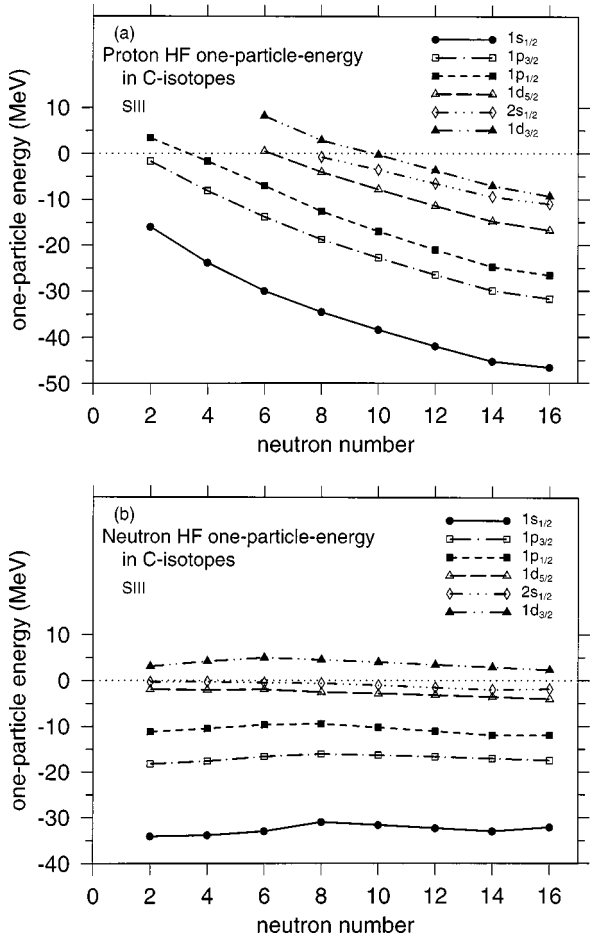

FIG. 1. One-particle spectra of C isotopes as a function of the neutron number, which are calculated in the HF approximation with the *S*III interaction: (a) for protons and (b) for neutrons. The positive one-particle energies express the resonant energies at which the calculated phase shift increases through $(1/2)\pi$.

III. ONE-PARTICLE LEVEL SCHEME OF C ISOTOPES

Since in the present work we are interested in spin-isospin modes, we choose the Skyrme interactions *S*III and *SG*II, which are effectively repulsive not only in the $(\vec{\sigma}\cdot\vec{\sigma})(\vec{\tau}\cdot\vec{\tau})$ channel but also in the $(\vec{\sigma}\cdot\vec{\sigma})$ channel. The Landau-Migdal parameters of the two interactions are found for the spin- and spin-isospin channels to be $G_0=0.052$ (0.011) and $G_0'=0.460$ (0.503) for *S*III (*SG*II) interaction, respectively. It is noted that experimental data of nuclear binding energies and radii, which are traditionally used in the determination of Skyrme parameters, are not very sensitive to the parameters in spin-isospin channels. Among those Skyrme interactions chosen, we find that the *S*III interaction gives ${}^{8}_{6}\text{C}_2$ and ${}^{22}_{6}\text{C}_{16}$ as the proton and neutron drip line nucleus of C isotopes, respectively, while the SGII interaction gives ${}^{8}_{6}\text{C}_2$ and ${}^{26}_{6}\text{C}_{20}$. Though those Skyrme interactions are not originally supposed to be employed for such light drip line nuclei, it is rather clear that the *SG*II interaction produces a too strong binding in C isotopes.

In Fig. 1 we show the proton and neutron HF one-particle energies of C isotopes calculated by using the *S*III interac-

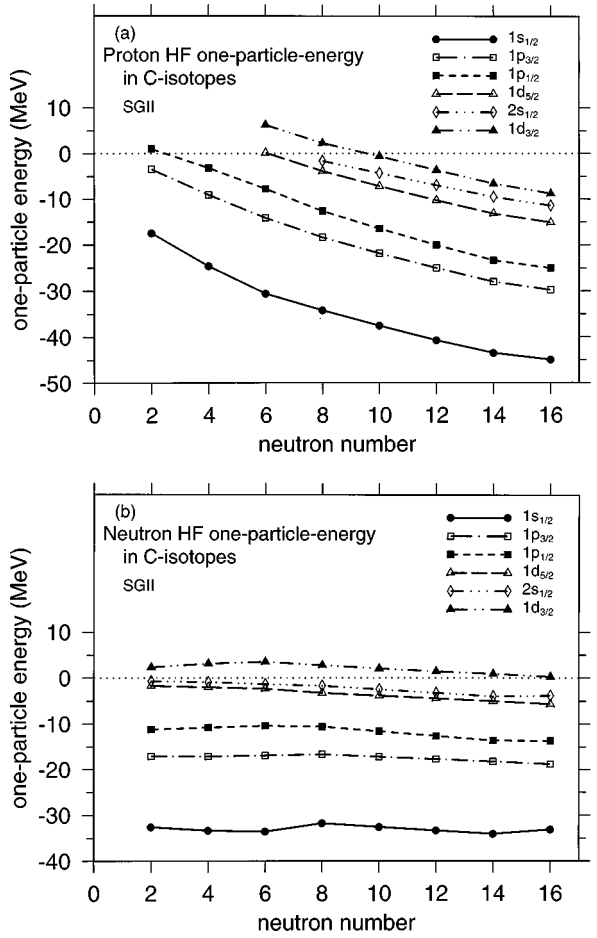

FIG. 2. One-particle spectra of C isotopes as a function of the neutron number, which are calculated in the HF approximation with the *SG*II interaction: (a) for protons and (b) for neutrons. See the caption to Fig. 1.

tion as a function of the neutron number, while in Fig. 2 those estimated by employing the *SG*II interaction. The positive one-particle energies plotted express the calculated energies of resonant states, at which the calculated phase shift increases through $(1/2)\pi$. We note that from the left edge (^{8}C) to the right edge (^{22}C) in Figs. 1 and 2 the mass number varies almost by a factor 3. The proton $1p_{1/2}$-$1p_{3/2}$ energy splitting obtained by using the *S*III (*SG*II) interaction is 5.09, 6.82, and 5.11 MeV (4.44, 6.38, and 4.71 MeV) for $^{8}_{6}C_2$, $^{12}_{6}C_6$, and $^{22}_{6}C_{16}$, respectively. It is seen that going from $^{12}_{6}C_6$ to $^{22}_{6}C_{16}$ the calculated proton $1p_{1/2}$-$1p_{3/2}$ energy splitting decreases appreciably stronger than $A^{-1/3}$, because the proton one-particle potential becomes slightly deeper and much more diffused, as the neutron number increases and approaches that of the drip line. Going from the β stable nucleus $^{12}_{6}C_6$ to the proton drip line nucleus $^{8}_{6}C_2$, the proton $1p_{1/2}$-$1p_{3/2}$ energy splitting also decreases appreciably, namely varies in the direction opposite to the $A^{-1/3}$ dependence. The decrease comes from the reduced probability of the $1p_{3/2}$ and $1p_{1/2}$ proton wave functions around the nuclear surface where the spin-orbit potential is effective, as the binding energy of the one-particle levels becomes smaller. In Fig. 3 we illustrate this situation by comparing the proton

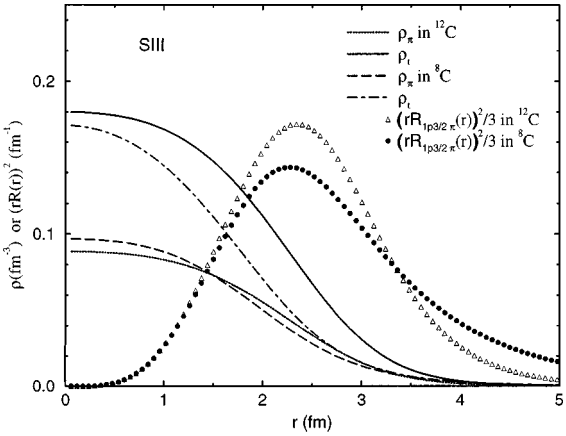

FIG. 3. The proton and total density of ^{12}C and ^{8}C calculated in the HF approximation with the *S*III interaction. Calculated $1p_{3/2}$ proton radial wave functions squared times r^2 are also shown for both ^{12}C and ^{8}C.

density, the total density, and the squared $1p_{3/2}$ one-proton wave function of $^{8}_{6}C_2$ with those of $^{12}_{6}C_6$. Since $Z=6$ is not a large number, the Coulomb barrier for C isotopes is not yet very high. Therefore the proton $1p_{3/2}$ wave function of $^{8}_{6}C_2$ can relatively easily extend to the outside of nuclei.

The neutron one-particle levels shown in Figs. 1(b) and 2(b) should be more carefully interpreted, since the occupation of the levels changes as the neutron number increases. Since neither the $1d_{5/2}$ level nor the $1d_{3/2}$ level is occupied in both $^{12}_{6}C_6$ and $^{8}_{6}C_2$, we may compare the neutron $1d_{3/2}$-$1d_{5/2}$ energy splitting. The splitting estimated by the *S*III (*SG*II) interaction is 5.03 and 6.95 MeV (4.03 and 5.83 MeV) for $^{8}_{6}C_2$ and $^{12}_{6}C_6$, respectively. The smaller splitting in $^{8}_{6}C_2$ comes mainly from the fact that for $r>2$ fm the proton density and thus the total density in $^{8}_{6}C_2$ decrease much more slowly than those in $^{12}_{6}C_6$. Consequently, the neutron one-particle resonant $1d_{3/2}$ state in $^{8}_{6}C_2$ feels a weaker spin-orbit potential.

IV. MAGNETIC DIPOLE EXCITATIONS OF $A=8$ MIRROR NUCLEI

The HF one-particle energy for the neutron $1p_{3/2}$ and $1p_{1/2}$ orbital in $^{8}_{2}He_6$ is -4.36 and $+0.60$ (-6.17 and -1.12) MeV, respectively, for the *S*III (*SG*II) interaction. Thus the spin-orbit splitting is nearly the same (4.96 and 5.05 MeV) for both interactions. In Fig. 4 we show the calculated unperturbed (free) and RPA response of $^{8}_{2}He_6$ to the $M1$ field. Since we use $g_l=0$ for neutrons, the response strength comes only from the spin contribution. The unperturbed peak slightly below 5 MeV for the *S*III interaction is of a resonance character rather than the threshold strength, while for the *SG*II interaction the position of the unperturbed peak below the threshold is indicated by the vertical dashed line. After including the RPA spin correlation a relatively broad peak is obtained for the *S*III interaction, while for the *SG*II interaction the RPA repulsive spin correlation pushes up the strength below the threshold to above. The RPA peak

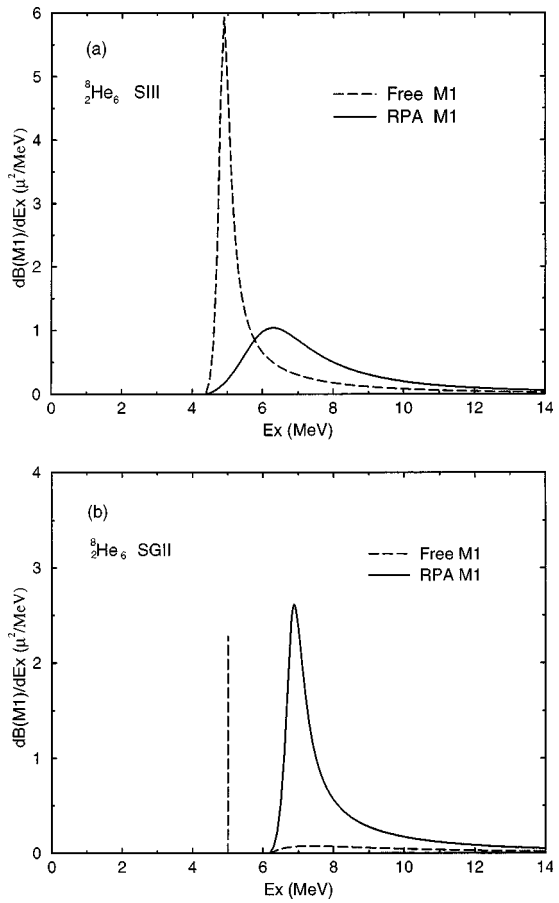

FIG. 4. Unperturbed (free) and RPA $M1$ strength function in ^{8}He calculated using the: (a) SIII and (b) SGII interaction. The $M1$ operator is defined in Eqs. (9) and (10) in units of $\mu = e\hbar/2m_pc$. The vertical dashed line at 5.05 MeV in (b) shows the position of the unperturbed energy of the neutron $(1p_{3/2} \rightarrow 1p_{1/2})_\nu$ excitation, which has no width since both the particle and hole state are bound states. The height of the vertical line is arbitrary.

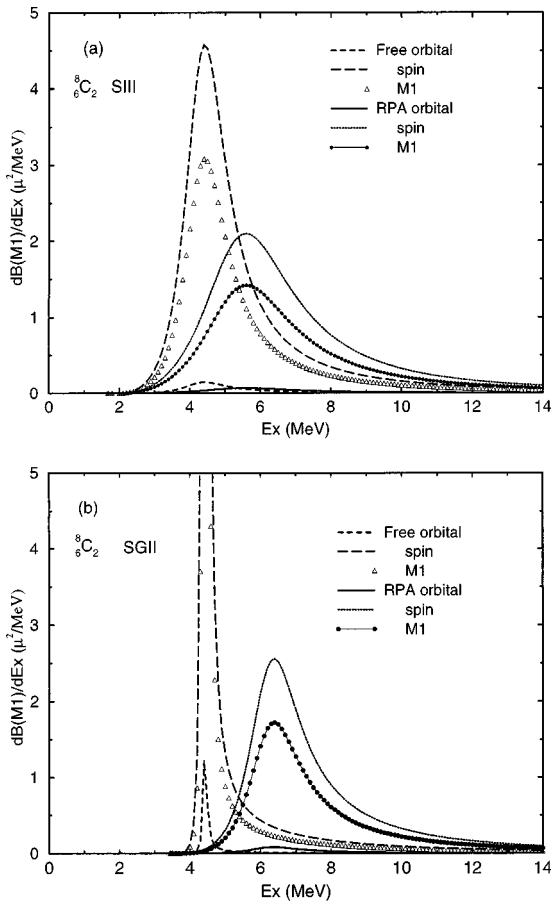

FIG. 5. Unperturbed (free) and RPA orbital, spin and $M1$ strength function in ^{8}C calculated using the (a) SIII and (b) SGII interaction. The $M1$ operator is defined in Eqs. (9) and (10) in units of $\mu = e\hbar/2m_pc$.

energy is 6.3 (6.9) MeV for the SIII (SGII) interaction.

In Fig. 5 the response functions of $^{8}_{6}C_{2}$ are shown. Since the response strength comes from the proton $1p_{3/2} \rightarrow 1p_{1/2}$ excitation, the $M1$ response function consists of the spin and orbital contribution. For the SIII (SGII) interaction the proton $1p_{3/2}$ state lies at -1.68 (-3.45) MeV, while the proton $1p_{1/2}$ state is a resonant state at 3.41 (0.99) MeV with the width of about 6.5 (0.16) MeV, respectively. The peak of the unperturbed strength for the SGII interaction is found almost exactly at $0.99-(-3.45)=4.44$ MeV, while that for the SIII interaction lies about 0.6 MeV lower than the estimate of p-h excitation, $3.41-(-1.68)=5.09$ MeV. The lowering of the peak energy is the result of the interference between the small background strength and the excitation involving the one-particle $1p_{1/2}$ resonant state with the extremely large width. The RPA response function has a peak at 5.6 (6.4) MeV for the SIII (SGII) interaction, with a broader shape for the SIII interaction. The peak energy of the RPA response in $^{8}_{6}C_{2}$ is lower than that in $^{8}_{2}He_{6}$ by 0.5–0.7 MeV, which is almost equal to the difference of the unperturbed spin-orbit $(1p_{1/2}-1p_{3/2})$ splitting. Due to the nature of the spin-flip excitation, $1p_{3/2} \rightarrow 1p_{1/2}$, the orbital contribution to the $M1$ response, which is proportional to $(g_s-g_l)^2$, is relatively small. Since only one configuration is contributing in essence, the spin and orbital RPA response are approximately proportional to each other at all energies.

The RPA calculations of the β-stable nucleus $^{12}_{6}C_{6}$ in the present model give the IV collective 1^+ state at $Ex \approx 10$ MeV. The presence of the deformation in $^{12}_{6}C_{6}$ pushes up the 1^+ state to the observed energy at $Ex = 15.1$ MeV. Based on the knowledge of 1^+ states in $^{12}_{6}C_{6}$, one might have expected that in the present $A=8$ mirror nuclei the strong M1 strength would lie certainly above 10 MeV. Thus the presence of the peak of the $M1$ strength below 7 MeV in the present calculation is unexpected. The calculated lower peak comes partly from the appreciably smaller spin-orbit splitting in the $A=8$ drip line nuclei and partly from the small number of particles participating in the excitation.

V. SPIN-ISOSPIN AND MAGNETIC DIPOLE EXCITATIONS OF $^{22}_{6}C_{16}$

In Fig. 6 the unperturbed and RPA response of $^{22}_{6}C_{16}$ to the $M1$ field is plotted as a function of the excitation energy. For the SIII [SGII] interaction the unperturbed response

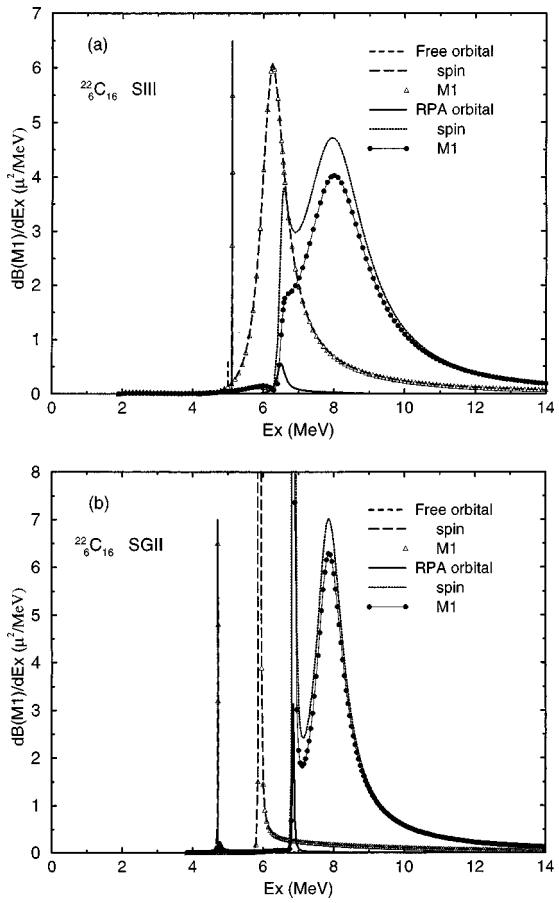

FIG. 6. Unperturbed (free) and RPA orbital, spin, and $M1$ strength function in ^{22}C calculated using the (a) SIII and (b) SGII interaction. The $M1$ operator is defined in Eqs. (9) and (10) in units of $\mu = e\hbar/2m_pc$. The vertical lines at 5.11 MeV in (a) and at 4.71 MeV in (b) show the positions of unperturbed energies of the deeply bound proton excitation $(1p_{3/2} \rightarrow 1p_{1/2})_\pi$, which has both the orbital and spin contribution to the $M1$ strength.

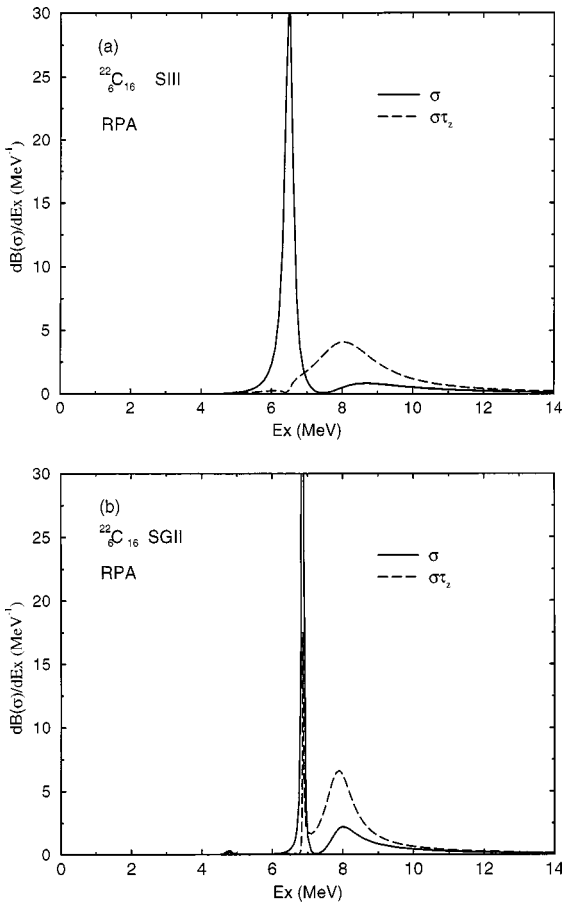

FIG. 7. RPA spin and spin-isospin strength function in ^{22}C using the (a) SIII and (b) SGII interaction. The operators are defined in Eqs. (11) and (12).

consists of the deeply bound proton $1p_{3/2} \rightarrow 1p_{1/2}$ excitation at $-26.61-(-31.72)=5.11$ $[-25.08-(-29.79)=4.71]$ MeV and the bound-to-resonant neutron $1d_{5/2} \rightarrow 1d_{3/2}$ excitation at $2.30-(-4.07)=6.37$ $[0.24-(-5.66)=5.90]$ MeV. After including the RPA spin correlation, the two-peak structure in the response function remains, though the higher peak receives a larger strength due to the repulsive nature of the interactions in both the $(\vec{\sigma}\cdot\vec{\sigma})(\vec{\tau}\cdot\vec{\tau})$ and $(\vec{\sigma}\cdot\vec{\sigma})$ channel. Most of the orbital contribution coming from the proton excitation remains in the lower RPA peak, though the wave function of the higher-lying peak indeed contains a non-negligible amount of the proton component, as seen from the appreciable difference between the σ and $\sigma\tau_z$ strength in Fig. 7. In the energy region lower than the two RPA peaks where the orbital response is still very weak, it is seen that the spin and orbital response contribute constructively to the $M1$ strength. In all other energy regions they contribute destructively in agreement with the unperturbed proton $1p_{3/2} \rightarrow 1p_{1/2}$ excitation. For both the SIII and SGII interaction a large $M1$ peak appears around 8 MeV, with a considerable tail on the high energy side.

In Fig. 7 the RPA response of $^{22}_{6}C_{16}$ to the spin and spin-isospin field, Eqs. (11) and (12), is shown, which may be of interest in nuclear reactions instead of electromagnetic fields. The peak positions of respective response can be already seen in Fig. 6. In both SIII and SGII the interaction is more strongly repulsive in the $(\vec{\sigma}\cdot\vec{\sigma})(\vec{\tau}\cdot\vec{\tau})$ channel than in the $(\vec{\sigma}\cdot\vec{\sigma})$ channel. Thus the response to the $\vec{\sigma}$ field has a peak energetically lower than that of the $\vec{\sigma}\tau_z$ field. The calculated response to the $\vec{\sigma}$ field contains possibly an appreciable ambiguity, since the Skyrme interaction in the $(\vec{\sigma}\cdot\vec{\sigma})$ channel is not accurately determined. For example, the SkM^* interaction which is often used in the market is attractive in that channel. In both Figs. 7(a) and 7(b) the lower peak of the $\sigma\tau_z$ strength comes from the proton contribution, while the higher peak from the neutron contribution. Since the proton spin excitation consists of the deeply bound one-particle wave functions, the coupling of it with the neutron spin excitation is rather weak. The weak coupling due to the difference between the neutron and proton wave functions is a general feature in drip line nuclei. Since the large RPA peak of the σ strength lies energetically close to the unperturbed neutron $1d_{5/2} \rightarrow 1d_{3/2}$ excitation, we examine the collective nature of the higher-lying RPA peak of the $\sigma\tau_z$ strength. When we take the ratio of the σ strength to the $\sigma\tau_z$ strength

lying in the region of $7.2<Ex<10$ MeV, we obtain 0.21 and 0.37 for the *S*III and *SG*II interaction, respectively. The obtained ratio may be compared with the value

$$\left[\frac{\sum_i^{(n)}\langle i|\sigma_z|0\rangle^2-\sum_i^{(p)}\langle i|\sigma_z|0\rangle^2}{\sum_i^{(n)}\langle i|\sigma_z|0\rangle^2+\sum_i^{(p)}\langle i|\sigma_z|0\rangle^2}\right]^2=\frac{4}{49}=0.08. \quad (14)$$

The ratio (14) is obtained from the RPA calculation only with the separable $(\vec{\sigma}\cdot\vec{\sigma})(\vec{\tau}\cdot\vec{\tau})$ interaction on the assumption that the unperturbed energy of the proton $1p_{3/2}\rightarrow 1p_{1/2}$ excitation is equal to that of the neutron $1d_{5/2}\rightarrow 1d_{3/2}$ excitation. The value (14) is appreciably smaller than the ratio of the IS quadrupole strength lying under the IV quadrupole giant resonance, $[(N-Z)/A)^2=[(16-6)/22]^2=25/121=0.21$, which is obtained from a similar model calculation including only the IV quadrupole RPA correlation with the degenerate unperturbed neutron and proton excitations. See Ref. [13]. It is clear that our calculated large ratio of the σ strength to the $\sigma\tau_z$ strength around the RPA peak of the $\sigma\tau_z$ strength comes from the dominance of neutron components in the excitation. In the present ${}^{22}_{6}C_{16}$ case the dominance of the neutron component comes not only from the larger strength of the neutron spin excitation but also from the higher unperturbed energy of the neutron excitation as well as the weak coupling between the neutron and proton spin excitations. For $Ex>12$ MeV the strength consists exclusively of the neutron excitation and thus the σ strength coincides with the $\sigma\tau_z$ strength.

The excitation energy 8 MeV of the calculated higher-lying peak of the $M1$ (or $\sigma\tau_z$) response in ${}^{22}_{6}C_{16}$ is compared with about 10 MeV in ${}^{12}_{6}C_6$, which is obtained from the same type of calculations. The ratio of 10/8 is approximately equal to $(12/22)^{-1/3}$. From Figs. 1(a) and 2(a) it is seen that going from ${}^{12}_{6}C_6$ to ${}^{22}_{6}C_{16}$ the proton $1p_{1/2}-1p_{3/2}$ energy splitting decreases stronger than the ratio $(12/22)^{-1/3}$; 6.82 (6.38) MeV in ${}^{12}_{6}C_6$ and 5.11 (4.71) MeV in ${}^{22}_{6}C_{16}$ for the *S*III (*SG*II) interaction. On the other hand, the neutron $1d_{3/2}-1d_{5/2}$ energy splitting in ${}^{22}_{6}C_{16}$ decreases weaker than the ratio $(12/22)^{-1/3}$ compared with the $1p_{1/2}-1p_{3/2}$ energy splitting in ${}^{12}_{6}C_6$; 6.37 (5.90) MeV in ${}^{22}_{6}C_{16}$ for the *S*III (*SG*II) interaction. When the RPA correlation is taken into account, the difference between the two unperturbed excitations is averaged out and we obtain approximately the $A^{-1/3}$ dependence.

VI. DISCUSSION AND CONCLUSION

Including simultaneously both the IS and IV spin correlation, the self-consistent RPA response function with Skyrme interactions is estimated in the coordinate space. As numerical examples we have chosen the *S*III and *SG*II interaction, which are repulsive in both the $(\vec{\sigma}\cdot\vec{\sigma})(\vec{\tau}\cdot\vec{\tau})$ and $(\vec{\sigma}\cdot\vec{\sigma})$ channel. The spin-orbit splitting, which plays a key role in the spin-dependent response functions, is found to become small for low angular momentum orbitals, as one-particle binding energies decrease considerably from the separation energy of β-stable nuclei.

The $1p_{1/2}-1p_{3/2}$ spin-orbit splitting in the HF calculations of the light mirror nuclei, ${}^{8}_{6}C_2$ and ${}^{8}_{2}He_6$, is about 30% smaller than the one in the β-stable nucleus ${}^{12}_{6}C_6$. Consequently, we have obtained the peak of the RPA $M1$ response at 5.6 (6.4) MeV for ${}^{8}_{6}C_2$ and 6.3 (6.9) MeV for ${}^{8}_{2}He_6$, for the *S*III (*SG*II) interaction. The obtained peak energies are much lower than those expected from our knowledge of the β-stable nucleus ${}^{12}_{6}C_6$.

We have estimated the $M1$, $\vec{\sigma}$, and $\vec{\sigma}\tau_z$ RPA response of the neutron drip line nucleus ${}^{22}_{6}C_{16}$. Corresponding to the unperturbed two-peak (the spin-flip excitations in the proton-*p* and neutron-*d* orbitals) structure, two $M1$ RPA peaks appear in the continuum. The higher-lying peak, which gets a larger $M1$ strength, is obtained around 8 MeV with an appreciable tail on the higher energy side. The dominance of the neutron configuration at the peak of the $\vec{\sigma}\tau_z$ response estimated around 8 MeV is understood as a feature of the neutron drip line nucleus. The σ strength obtained under the $\sigma\tau_z$ peak is much stronger than the simple estimate (14). The dominance by the neutron component at the $\sigma\tau_z$ peak is due not only to the weak coupling between the neutron and proton excitations but also to a non-negligible difference between the unperturbed energies.

ACKNOWLEDGMENTS

One of the authors (H.S.) acknowledges the financial support provided by The Swedish Foundation for International Cooperation in Research and Higher Education (STINT), which makes it possible for him to work at the Lund Institute of Technology.

[1] I. Hamamoto, H. Sagawa, and X.Z. Zhang, Phys. Rev. C **55**, 2361 (1997); Nucl. Phys. **A626**, 669 (1997); Phys. Rev. C **56**, 3121 (1997); **57**, R1064 (1998); Nucl. Phys. **A648**, 203 (1999).
[2] F. Catara, C.H. Dasso, and A. Vitturi, Nucl. Phys. **A602**, 181 (1996).
[3] F. Catara, E.G. Lanza, M.A. Nagarajan, and A. Vitturi, Nucl. Phys. **A614**, 86 (1997); **A624**, 449 (1997).
[4] A. Bohr and B.R. Mottelson, *Nuclear Structure* (Benjamin, Reading, MA, 1969), Vol. I, Chap. 2.
[5] I. Hamamoto and X.Z. Zhang, Phys. Rev. C **58**, 3388 (1998).
[6] I. Hamamoto, H. Sagawa, and X.Z. Zhang, Phys. Rev. C **53**, 765 (1996).
[7] L.S. Ferreira, E. Maglione, and R.J. Liotta, Phys. Rev. Lett. **78**, 1640 (1997); L.S. Ferreira and E. Maglione, private communication.
[8] G.F. Bertsch and S.F. Tsai, Phys. Rep. **18**, 125 (1975).
[9] S. Shlomo and G.F. Bertsch, Nucl. Phys. **A243**, 507 (1975).
[10] K.F. Liu and Nguyen Van Giai, Phys. Lett. **65B**, 23 (1976).
[11] Appendix 3A of Ref. [4].
[12] Nguyen Van Giai and H. Sagawa, Phys. Lett. **106B**, 379 (1981).
[13] I. Hamamoto, Phys. Rev. C **60**, 031303 (1999).